ELSEVIER

Journal of Molecular Structure (Theochem) 499 (2000) 1–12

THEO CHEM

www.elsevier.nl/locate/theochem

Comment on the mechanism of proton-coupled electron transfer reactions

Sang-Ik Cho, Seokmin Shin*

Department of Chemistry and Center for Molecular Catalysis, Seoul National University, Seoul 151-742, South Korea

Received 28 December 1998; accepted 2 July 1999

Abstract

We present detailed studies of the mechanism of proton-coupled electron transfer (PCET) reactions based on the recently proposed one-dimensional model system by Fang and Hammes-Schiffer [J. Chem. Phys. 106 (1997) 8442]. Three different mechanisms: a concerted ET–PT mechanism, a sequential PT → ET mechanism, and a sequential ET → PT mechanism, have been suggested. We have examined the dynamical coupling between the proton and electron degrees of freedom, which is responsible for subtle differences in various PCET reaction mechanisms. For the concerted ET–PT and the sequential ET → PT mechanisms, the dynamics of the quantum wavepackets for the combined proton–electron system are consistent with proposed mechanisms. In contrast, for the sequential PT → ET mechanism, it is found that the electron transfer (ET) apparently happens prior to the proton transfer (PT) for the conditions adopted in the present calculations. The different dynamical behavior of the PT → ET and ET → PT mechanisms is partially attributed to the time-scale differences arising from the mass disparity of the proton and electron.

Keywords: Proton transfer; Electron transfer; PCET; Quantum dynamics; Multiple time-scale

1. Introduction

The coupling of proton motion to electron transfer (ET) has been found to play an important role in biological and chemical energy conversions. In the proteins involved in photosynthesis and respiration, the charge separation induced by the ET serves as the driving force for the proton transfer (PT) [1–6]. In other proteins, the movement of electrons is closely related to the hydrogen-bonded structures [7,8]. To elucidate such proton-coupled electron transfer (PCET) processes, biomimetic systems such as dicarboxylic acids, which form an intramolecular donor/acceptor ET couple separated by a proton interface, have been studied experimentally [9,10]. Cukier and coworkers [11–15] have carried out extensive theoretical studies on such systems. They have provided insights on the mechanism and physical principles of PCET reactions. In PCET, the electron and proton may transfer consecutively, or they may transfer concertedly. By using dielectric continuum theory to obtain the proton-solvated surfaces, they developed methods for calculating the rate constants for the several reaction complexes.

Recently, Hammes-Schiffer and coworkers [16–18] have proposed a simple-model PCET reactions. The model consists of three coupled degrees of freedom that represent an electron, a proton, and a solvent coordinate. The general model system is closely related to the minimal model for a charge transfer

* Corresponding author. Tel.: + 82-2-880-6639; fax: + 82-2-889-1568.

E-mail address: sshin@plaza.snu.ac.kr (S. Shin).

0166-1280/00/$ - see front matter
PII: S0166-1280(99)00273-0

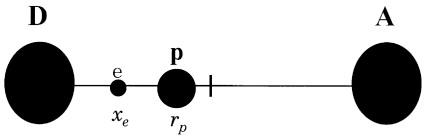

Fig. 1. Schematic diagram of the one-dimensional model system for PCET. The donor (*D*) and acceptor (*A*) are separated by a fixed distance. The system is described by the position of the electron (*e*), x_e, and proton (*p*), r_p. The origin for the coordinates is defined as the midpoint of the *D–A* axis.

reaction studied by one of the authors [19]. It was found that a wide range of PCET dynamics could be obtained by altering the parameters in the model. They suggested three different mechanisms: a concerted mechanism in which the proton and electron are transferred simultaneously; sequential mechanisms in which either the proton or the electron is transferred prior to the other. A surface-hopping method, namely molecular dynamics with quantum transitions (MDQT) developed by Tully et al. [20,21], was applied to model systems where nonadiabatic transitions between the mixed proton/electron adiabatic quantum states were incorporated. It was found that nonadiabatic effects are important in determining the rates and mechanisms of PCET reactions.

In this paper, we present an analysis of the PCET model proposed by Fang and Hammes-Schiffer (FHS) [16]. Our analysis is based on exact quantum-mechanical wavepacket propagations for the combined electron–proton dynamics. The nonadiabatic MD simulations used by FHS relied on a semiclassical surface-hopping procedure. In those schemes, the proton and electron degrees of freedom are treated equivalently in spite of their mass disparity. The motivation for the present study is to examine the dynamical coupling between the electron and proton degrees of freedom responsible for the detailed mechanism of PCET reactions. The main focus will be on the feasibility of various mechanisms suggested for PCET dynamics.

The paper is organized as follows. The definition of the theoretical model and a brief description of the computational scheme for the dynamics of the system are given in Section 2. The results are presented in Section 3, and Section 4 summarizes the conclusions together with some discussion.

2. Theory

The general model system for PCET reactions consists of three coupled degrees of freedom: an electron coordinate x_e, a proton coordinate r_p, and a solvent coordinate R. This model system, which is related to the minimal model of a charge transfer reaction by Shin and Metiu [19], was described in detail in Ref. [16]. The electron donor (*D*) and acceptor (*A*) are separated by a fixed distance and the electron and proton are considered to move in one dimension along the *D–A* axis (Fig. 1). In our case, the coordinates for the electron and proton are defined with respect to the origin defined as the center of the *D–A* axis. The solvent coordinate, representing a collective solvent mode, is linearly coupled to the proton and electron and provides a driving force for the PCET.

The Hamiltonian for the model system is given by

$$H = \frac{P_s^2}{2M_s} + V_s(R) + H_{pe}(r_p, r_e, R), \tag{1}$$

where the proton–electron Hamiltonian, H_{pe}, is defined as

$$H_{pe} = -\frac{\hbar^2}{2m_p}\frac{\partial^2}{\partial r_p^2} - \frac{\hbar^2}{2m_e}\frac{\partial^2}{\partial x_e^2} + V_p(r_p) + V_e(x_e) + V_{pe}(r_p, x_e) + V_{pes}(r_p, x_e, R). \tag{2}$$

The detailed forms of the potential models are given in the original model by FHS. Changing the parameters in the potential model will lead to different mechanisms for PCET dynamics.

The solvent potential is the simple harmonic oscillator potential

$$V_s(R) = \tfrac{1}{2}M_s\omega_s^2(R - R_0)^2, \tag{3}$$

where the mass M_s is chosen to be 12.0 a.m.u. and the frequency ω_s of the collective solvent mode is chosen to be 80–90 cm^{-1}.

The proton potential is a double-well PT potential

represented by the quadratic polynomial

$$V_p(r_p) = \frac{12\Delta E}{(a_2 - a_1)^3(2a_3 - a_1 - a_2)} \times \left\{ \frac{r_p^4}{4} - (a_1 + a_2 + a_3)\frac{r_p^3}{3} + (a_1a_2 + a_1a_3 + a_2a_3)\frac{r_p^2}{2} - (a_1a_2a_3)r_p + \frac{a_2^2}{12}[a_2^2 - 2a_2(a_1 + a_3) + 6a_1a_3] \right\}, \quad (4)$$

where ΔE is the energy difference between the first minimum and the maximum, and a_1 and a_3 correspond to the positions of the two minima and a_2 to the position of the maximum ($a_3 > a_2 > a_1$). The maximum of the potential is defined to be zero.

The electron potential is the pseudopotential between the electron and its donor and acceptor. This form of the pseudopotential is more realistic and easier to handle computationally than either a coulomb potential or a simple semiempirical potential [19,22].

$$V_e(x_e) = -\frac{Q_eQ_D\ \mathrm{erf}(r_{eD}/\xi_{eD})}{r_{eD}} - \frac{Q_eQ_A\ \mathrm{erf}(r_{eA}/\xi_{eA})}{r_{eA}}, \quad (5)$$

where Q_e, Q_D and Q_A are the absolute values of the effective charges on the electron, the donor and the acceptor, and r_{eD} and r_{eA} are the distances between the electron and the donor and acceptor, respectively. For numerical efficiency, a repulsive term with the exponential form is included to prevent the electron from traveling too far beyond the donor and acceptor.

The electron–proton interaction is also treated as a pseudopotential interaction

$$V_{pe}(r_p, x_e) = -\frac{Q_pQ_e\ \mathrm{erf}(r_{pe}/\xi_{pe})}{r_{pe}}, \quad (6)$$

where r_{pe} is the distance between the electron and proton.

The linear coupling between the solute (proton + electron) and the polarization field of the solvent is given as

$$V_{pes}(r_p, x_e, R) = -C_{sp}(R - R_p^0)(r_p - r_p^0) - C_{se}(R - R_e^0)(x_e - r_e^0), \quad (7)$$

where C_{sp} and C_{se} are the coupling constants and R_p^0, R_e^0, r_p^0 and r_e^0 are flexible parameters. The physical basis for this linear coupling is the interaction between the dipole moment of the solute and the polarization field of the solvent.

The motion of the solvent coordinate is followed classically while the combined proton–electron dynamics is described by quantum mechanics. This is done by the usual hybrid quantum/classical method based on the time-dependent Hartree approximation [23]. The initial wavefunction for the proton–electron system is obtained as the equilibrium configuration for a fixed solvent coordinate by the relaxation method. The quantum wavepacket is propagated by a multiple time step version of the split-operator method [24]. For the classical dynamics of the solvent, the equation of motion is solved by the velocity Verlet algorithm.

It is noted that the above mixed quantum/classical or Ehrenfest method uses a mean potential for the classical solvent coordinate. The limitations of such approaches are well known [21,25]. As pointed out by Fang and Hammes-Schiffer [16], mixed state methods may have difficulty in describing branching processes in charge transfer reactions. In this work, our main concern is the effect of coupling between the proton and electron degrees of freedom on the mechanism of PCET dynamics. In this regard, we assume that the mixed quantum/classical method can be used for our purposes, considering the approximate treatment of the solvent by one collective coordinate. We also note that the calculations presented here will refer mainly to cases where the solvent degree of freedom has enough energy to induce appreciable PCET reactions. In those cases, the dynamics of the system is found to follow the dominant channel path and the mean field approach should be reasonable. Recently, Kohen et al. [26] reported that the mean field mixed quantum/classical method displays useful accuracy in cases where linear couplings dominate. They studied models involving one light and one heavy degree of freedom and exhibiting substantial nonadiabatic behavior.

3. Results

As discussed in the paper by FHS, the model

Table 1
The parameters for the three mechanisms of the PCET reactions (all numbers are in atomic units)

Concerted ET–PT mechanism			
$M_s = 22\,000.0$	$R_0 = 0.0$	$\omega_s = 3.72 \times 10^{-4}$	$\Delta E = 1.2 \times 10^{-2}$
$a_1 = 2.5$	$a_2 = 3.0$	$a_3 = 3.5$	$d_{DA} = 6.0$
$Q_D = 0.6$	$Q_A = 0.6$	$Q_p = 0.32$	$Q_e = 0.32$
$C_{sp} = 2.0 \times 10^{-3}$	$C_{se} = 2.0 \times 10^{-3}$		
$r_p^0 = 3.0$	$r_e^0 = 3.0$	$R_p^0 = 0.0$	$R_e^0 = 0.0$
Sequential PT → ET mechanism			
$M_s = 22\,000.0$	$R_0 = -0.4$	$\omega_s = 4.0 \times 10^{-4}$	$\Delta E = 1.2 \times 10^{-2}$
$a_1 = 3.5$	$a_2 = 4.0$	$a_3 = 4.55$	$d_{DA} = 8.0$
$Q_D = 0.6$	$Q_A = 0.6$	$Q_p = 0.15$	$Q_e = 0.15$
$C_{sp} = 1.0 \times 10^{-2}$	$C_{se} = 2.0 \times 10^{-3}$		
$r_p^0 = 4.0$	$r_e^0 = 4.0$	$R_p^0 = -0.6$	$R_e^0 = 0.0$
Sequential ET → PT mechanism			
$M_s = 22\,000.0$	$R_0 = -0.3$	$\omega_s = 4.0 \times 10^{-4}$	$\Delta E = 1.2 \times 10^{-2}$
$a_1 = 3.5$	$a_2 = 4.0$	$a_3 = 4.5$	$d_{DA} = 8.0$
$Q_D = 0.55$	$Q_A = 0.55$	$Q_p = 0.15$	$Q_e = 0.15$
$C_{sp} = 3.0 \times 10^{-2}$	$C_{se} = 4.0 \times 10^{-3}$		
$r_p^0 = 4.0$	$r_e^0 = 4.0$	$R_p^0 = 0.0$	$R_e^0 = -0.6$

described in Section 2 can generate various mechanisms for PCET dynamics through the choice of different sets of parameters. They proposed three different PCET mechanisms: (i) a concerted PCET mechanism, in which the proton and electron are transferred simultaneously; (ii) a sequential mechanism, in which the PT occurs first, followed by the ET; and (iii) a sequential mechanism, in which the ET precedes the PT. We will denote the three mechanisms as ET–PT, PT → ET, and ET → PT, respectively. The parameters of the models were chosen to represent electron donor–acceptor pairs connected by a hydrogen-bonded interface [9,10]. We used the same parameter sets for the three proposed mechanisms as employed by FHS (Table 1).

The physical basis for the three PCET mechanisms can be understood by examining each term in the potential model. Table 2 explains the qualitative differences in the interaction potentials for the different PCET mechanisms. The interactions of the proton and electron with the donor and acceptor, as given by the double-well potential for the proton and the pseudopotential for the electron, can be either symmetric or asymmetric. The couplings of the solvent with the proton and electron, which will induce their transfer through solvent fluctuations, are characterized by the critical configurations for PT and ET. Such configurations can be either symmetric or asymmetric with respect to the midpoint of the axis between the donor and acceptor. For the concerted PCET mechanism (ET–PT), all the environments are symmetric. In addition, the strengths of the solvent couplings with the proton and electron are identical. Another important aspect is that the interaction between the proton and the electron is strong in this case. When the interaction potentials involving either the proton or electron become asymmetric, sequential mechanisms are obtained. In the model potential used for the PT → ET mechanism by FHS, the double-well potential of the proton is asymmetric, with the potential well at the acceptor side being lower in energy. The asymmetric solvent coupling with the proton will induce PT first,

Table 2
Characteristics of different interaction energy terms for the potential models of the three PCET reaction mechanisms

	$V_p(r_p)$	$V_e(x_e)$	e–s Coupling	p–s Coupling	e–p Coupling
ET–PT	Symmetric	Symmetric	Symmetric	Symmetric	Strong
PT → ET	Asymmetric	Symmetric	Symmetric	Asymmetric	Weak
ET → PT	Symmetric	Symmetric	Asymmetric	Symmetric	Weak

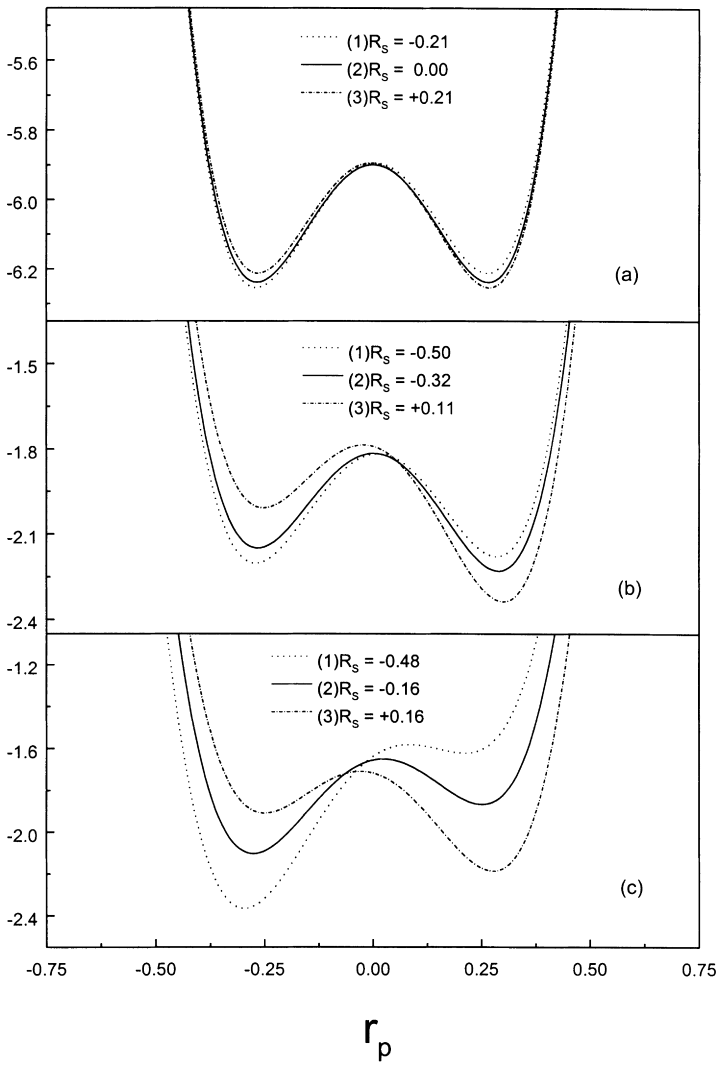

Fig. 2. The effective double-well potential of the proton transfer for (a) ET–PT, (b) PT → ET, and (c) ET → PT mechanisms. In each case, the three solvent coordinates represent sequential solvent configurations leading to PCET reactions.

while the electron is kept at the donor site by the symmetric solvent coupling. For the sequential ET → PT mechanism, only the coupling of the solvent with the electron was chosen to be asymmetric. The ET will be induced first by the solvent fluctuations for which the proton remains to be stabilized around the donor side. For both sequential mechanisms, the interaction between the proton and electron is weaker than that for the concerted ET–PT case.

The above discussion is based solely on the potential energy surfaces and minimum energy configurations. The proposed mechanisms for PCET dynamics can be inferred by locating the global minimum configurations on the two-dimensional potential energy surfaces for the proton and electron as a function of solvent coordinate. Similar conclusions can be reached by examining the *effective* double-well potential for the proton. The effective potential for the proton is defined by integrating the electronic degrees of freedom at a given solvent coordinate. In other words, for a fixed solvent configuration, we obtain the usual adiabatic PES for the proton. Fig. 2 shows

Table 3
Initial position and momentum of the solvent coordinate in the calculations for the dynamics of the three PCET reaction mechanisms

Mechanism	R_s^{ini} (Å)	P_0 (a.u.)
ET–PT	− 0.24	4.0
PT → ET	− 0.58	25.0
ET → PT	− 0.50	28.0

the effective double-well potentials of the proton for the three mechanisms considered. In the concerted ET–PT mechanism, the double-well potential is symmetric for the medium solvent configuration ($R_s = 0.0$), while slightly asymmetric for the negative ($R_s = -0.21$) and the positive ($R_s = +0.21$) solvent fluctuations. For the PT → ET mechanism, the double-well potential favors the proton being on the acceptor side even at $R_s = -0.32$. In contrast, the energy of the double-well potential on the acceptor side does not become lower until the solvent coordinate takes a positive value for the ET → PT mechanism. The actual dynamics of the system can be different from that predicted by considerations based on the minimum energy configurations on PES. The dynamics for the three parts of the system (electron, proton and solvent) have vastly different time-scales due to the large disparity in masses. Although the dynamics of the proton is considered on an equal footing with that of the electron, the intrinsic time-scale difference for the two motions will be reflected in the dynamical behavior of the system.

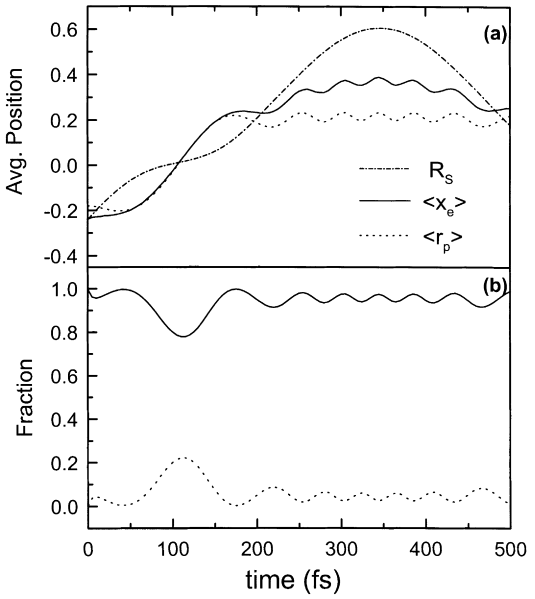

Fig. 3. (a) The position of the solvent, R_s (dot-dashed line: in Å), and the averaged positions of the electron, $\langle x_e \rangle = \langle \Phi | x_e | \Phi \rangle$ (solid line: in Å), and proton, $\langle r_p \rangle = \langle \Phi | r_p | \Phi \rangle$ (dotted line: in Å), as a function of time for the dynamics of ET–PT mechanism. (b) The fraction of the ground (solid line) and the first excited (dotted line) adiabatic states contained in the time-dependent wavefunction of the combined proton–electron system from the calculations as given in (a).

In the two-dimensional method [13], where both the proton and electron are treated quantum-mechanically as tunneling objects, one can define *adiabatic* states as a function of solvent coordinates. The adiabatic potential energy curves for the three mechanisms, which is the reproduction of the same figures given in the paper by FHS [16], can be obtained by the relaxation method based on the imaginary-time propagation of the two-dimensional wavepackets. For the ET–PT mechanism, the ground state potential has the form of a symmetric double-well potential, which is separated from the excited state by about 0.2 eV at the midpoint of the reaction path. The PCET reaction can proceed adiabatically in the ground state at lower energies or nonadiabatically with the excited state affecting the barrier crossing process. For both the sequential PT → ET and ET → PT mechanisms, the adiabatic surfaces show several strong nonadiabatic coupling regions as a function of solvent coordinate. It can be concluded that excited states may play an important role in PCET reactions. It is noted that the proton and electron degrees of freedom have very different excitation energies for corresponding quantum states. Obviously, the electronic excitation energy is much higher. Therefore, the excited adiabatic states mentioned above correspond to the excited states for the proton degree of freedom.

We have studied the dynamics of the system by two-dimensional wavepacket propagation for the combined proton–electron degree of freedom, while the solvent motion is treated classically for the three PCET mechanisms. The initial wavepacket is determined for the equilibrium configuration corresponding to the situation where both the proton and the electron are located at the donor side. With a positive momentum for the solvent coordinate, the

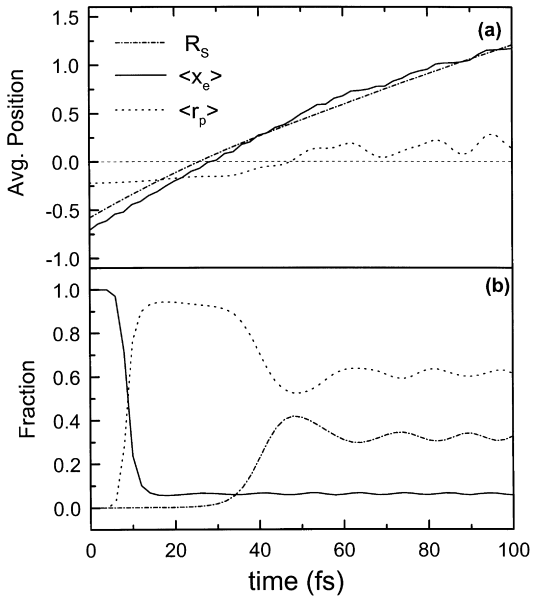

Fig. 4. (a) The position of the solvent, R_s (dot-dashed line: in Å), and the averaged positions of the electron, $\langle x_e\rangle = \langle \Phi|x_e|\Phi\rangle$ (solid line: in Å), and proton, $\langle r_p\rangle = \langle \Phi|r_p|\Phi\rangle$ (dotted line: in Å), as a function of time for the dynamics of PT → ET mechanism. A horizontal (dashed) line is drawn to show the position of the midpoint of both ET and PT along the donor–acceptor axis. (b) The fraction of the ground (solid line), the first excited (dotted line), and the second excited (dot-dashed line) adiabatic states contained in the time-dependent wavefunction of the combined proton–electron system from the calculations as given in (a).

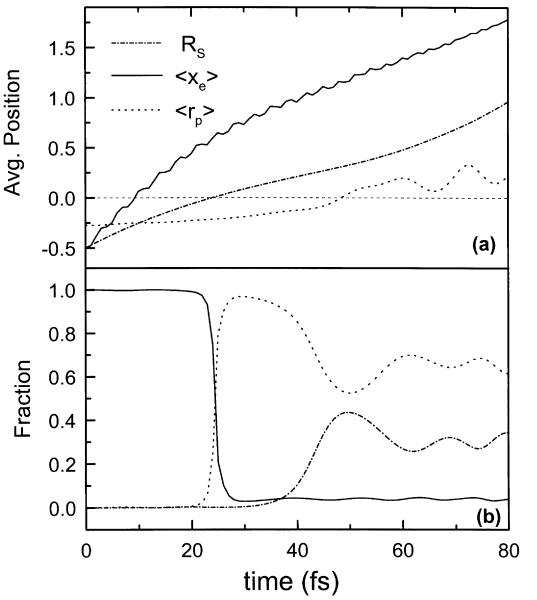

Fig. 5. (a) The position of the solvent, R_s (dot-dashed line: in Å), and the averaged positions of the electron, $\langle x_e\rangle = \langle \Phi|x_e|\Phi\rangle$ (solid line: in Å), and proton, $\langle r_p\rangle = \langle \Phi|r_p|\Phi\rangle$ (dotted line: in Å), as a function of time for the dynamics of ET → PT mechanism. A horizontal (dashed) line is drawn to show the position of the midpoint of both ET and PT along the donor–acceptor axis. (b) The fraction of the ground (solid line), the first excited (dotted line), and the second excited (dot-dashed line) adiabatic states contained in the time-dependent wavefunction of the combined proton–electron system from the calculations as given in (a).

configuration of the system will change toward states where both the proton and electron transfer is induced. We will consider the cases in which eventually both PT and ET are complete with sufficient energy for the solvent. Table 3 lists the initial configurations (positions) and momenta of the solvent used in the calculations for the three mechanisms. During the time evolution of the system, we have obtained the solvent configuration (R_s) from the classical trajectory, and the average positions for the proton ($\langle r_p\rangle$) and the electron ($\langle x_e\rangle$) as expectation values calculated from the time-dependent wavefunction. We have also calculated the fractions of the adiabatic states contained in the time-dependent wavepacket of the system.

Fig. 3 shows the results for the concerted ET–PT mechanism. The average positions for the proton and electron clearly demonstrate that they are transferred simultaneously. With a relatively small momentum ($P_0 = 4.0$ a.u.), the solvent is reflected back within the harmonic potential well at later times. For such a relatively low energy, the system mostly stays in the ground adiabatic state (Fig. 3(b)). It is noted that the mechanism in this case is similar to that in the 'adiabatic transfer' regime for the minimal model of charge transfer considered in the previous study [19].

For the PT → ET mechanism, it is found that a large initial momentum for the solvent coordinate is required for both the proton and electron to be transferred. With the value $P_0 = 25.0$ a.u., the results of our calculations showed different system behavior from that predicted by the sequential PT → ET mechanism. Fig. 4(a) shows that the electron is apparently transferred ahead of the proton. As expected, the excited states are found to be substantially involved. As early as about 10 fs, the system is switched to the first excited state and the second excited state is mixed in at $t \sim 40$ fs. In the ET → PT mechanism, a

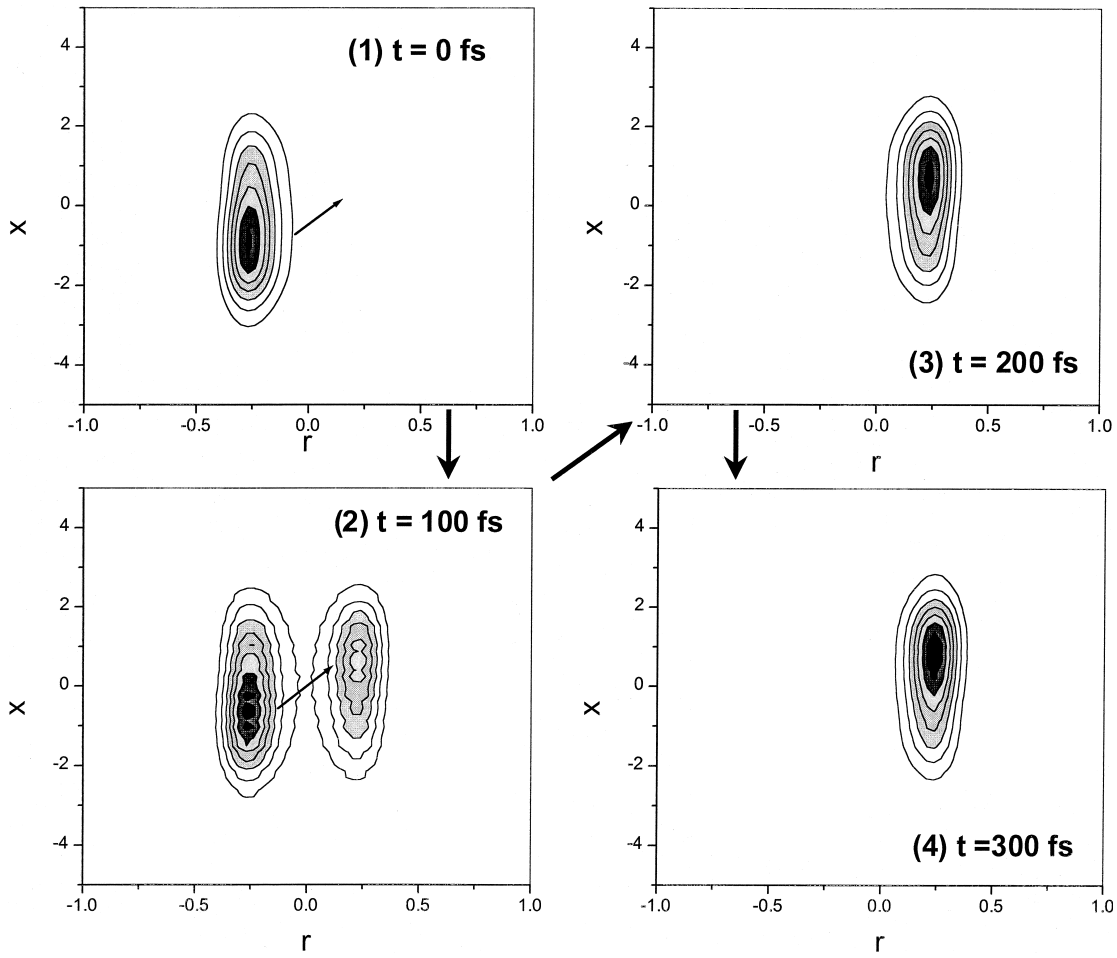

Fig. 6. The time-dependent wavepackets for the combined proton–electron dynamics of ET–PT mechanism. The units of the proton (r) and electron (x) coordinates are in Å. The arrows inside the figures represent the direction of subsequent movements of the wavepackets.

similarly large initial solvent momentum ($P_0 = 28.0$ a.u.) was used for the completion of the PCET reaction. As shown in Fig. 5(a), the electron is clearly transferred first in this case. The tunneling of the electron occurs while the system is in the ground adiabatic state (Fig. 5(b)). The PT at later times involves the excited states as in the case of PT → ET.

The different behavior of the system described above for the three mechanisms can also be seen from the time-dependence of the two-dimensional wavepackets for the combined proton–electron dynamics. For the concerted ET–PT (Fig. 6) and the sequential ET → PT (Fig. 8) mechanisms, the wavepacket motions are consistent with the proposed dynamics of the system. However, the wavepacket dynamics for the PT → ET mechanism (Fig. 7) showed that the proton is not transferred first. The two-dimensional tunneling paths for the three mechanisms are more clearly displayed by the trajectories defined by the average positions of the proton and electron (Fig. 9).

4. Conclusions

We have presented detailed studies on the mechanism of proton-coupled electron transfer (PCET) reactions based on the recently proposed one-dimensional

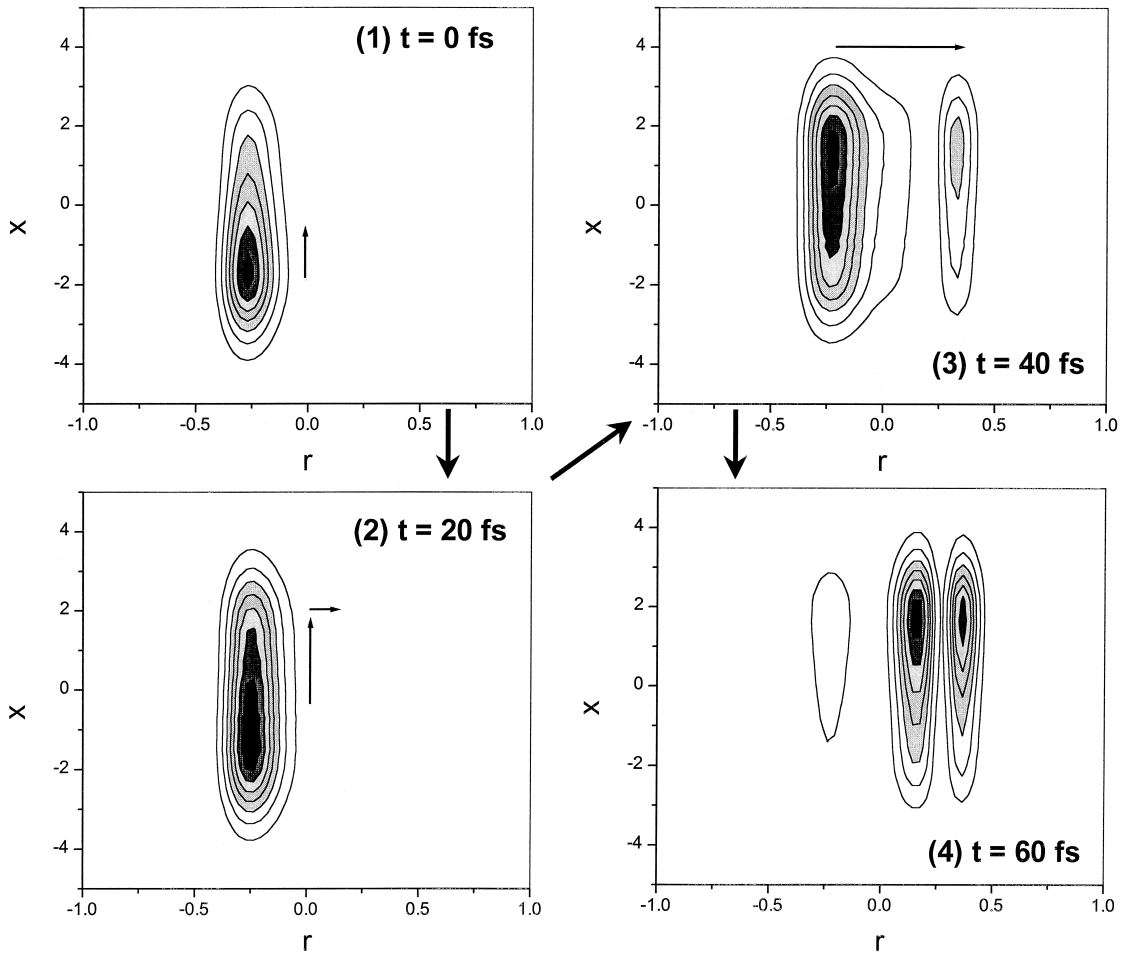

Fig. 7. The time-dependent wavepackets for the combined proton–electron dynamics of PT → ET mechanism. The units of the proton (r) and electron (x) coordinates are in Å. The arrows inside the figures represent the direction of subsequent movements of the wavepackets.

model. The model describes a wide range of PCET dynamics. Three different mechanisms: a concerted ET–PT mechanism, a sequential PT → ET mechanism, and a sequential ET → PT mechanism have been suggested. The PCET dynamics for the three cases have been studied previously by using a surface-hopping method [16,17]. Although the dynamical aspects of PCET reactions were inferred in those studies, more direct information on the detailed mechanism concerning quantum motions of the proton and electron should be useful. In this study, we have examined the dynamical coupling between the proton and electron degrees of freedom, which produces subtle differences in the detailed mechanism of PCET reactions.

The model consists of a proton, an electron, and a collective solvent coordinate. The motion of the solvent is treated classically while the combined proton–electron dynamics is described by quantum dynamics. The time-dependence of the wavepacket for the proton and electron degrees of freedom is used to examine the behavior of the system in different mechanisms. For the concerted ET–PT and the sequential ET → PT mechanisms, the dynamics of the quantum wavepackets are consistent with proposed mechanisms predicted from the potential models with appropriate parameter sets. In contrast,

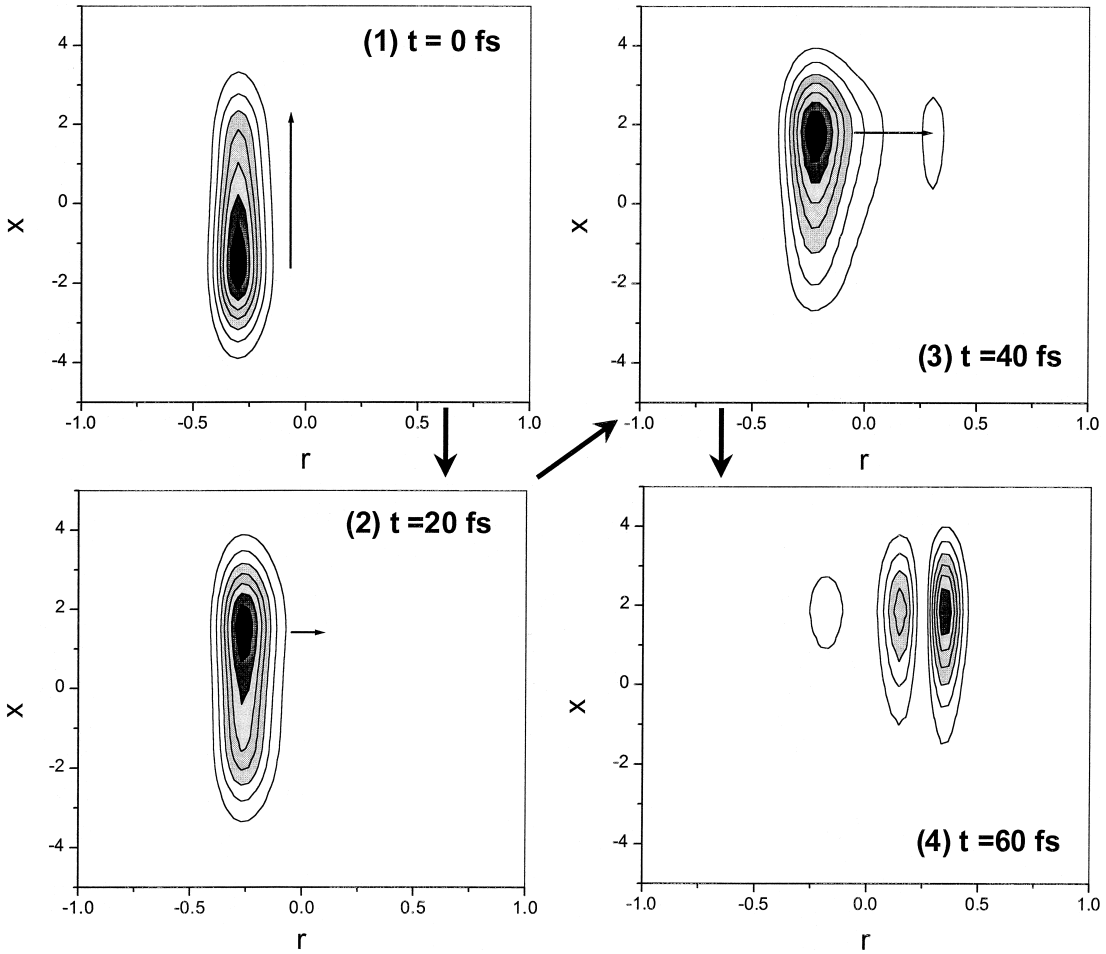

Fig. 8. The time-dependent wavepackets for the combined proton–electron dynamics of ET → PT mechanism. The units of the proton (r) and electron (x) coordinates are in Å. The arrows inside the figures represent the direction of subsequent movements of the wavepackets.

the sequential PT → ET mechanism showed different behavior. Although the potential model predicts the occurrence of PT ahead of ET, it is found from the wavepacket propagations that the ET apparently happens prior to the PT.

The different dynamical behavior of the PT → ET and ET → PT mechanisms reflects the time-scale differences arising from the mass disparity of the proton and electron. For a sequential (consecutive) mechanism to occur, other degrees of freedom other than the transferring (tunneling) degree of freedom need to be displaced *adiabatically* until a critical configuration induces the tunneling. The sequential ET → PT mechanism corresponds well to such a general scenario where the solvent and proton provide an appropriate environment for ET. In the PT → ET mechanism, tunneling of the proton with the electron configuration being fixed *adiabatically* does not constitute a reasonable picture. PT may not take place fast enough to take advantage of the instantaneous configuration favorable for the transfer. The adjustment of the electron to the proton motion can be much faster, resulting in the change of environment for PT. While PT is delayed, the electron may find an appropriate configuration for its transfer, resulting in ET prior to PT. The above discussion provides a reasonable explanation for

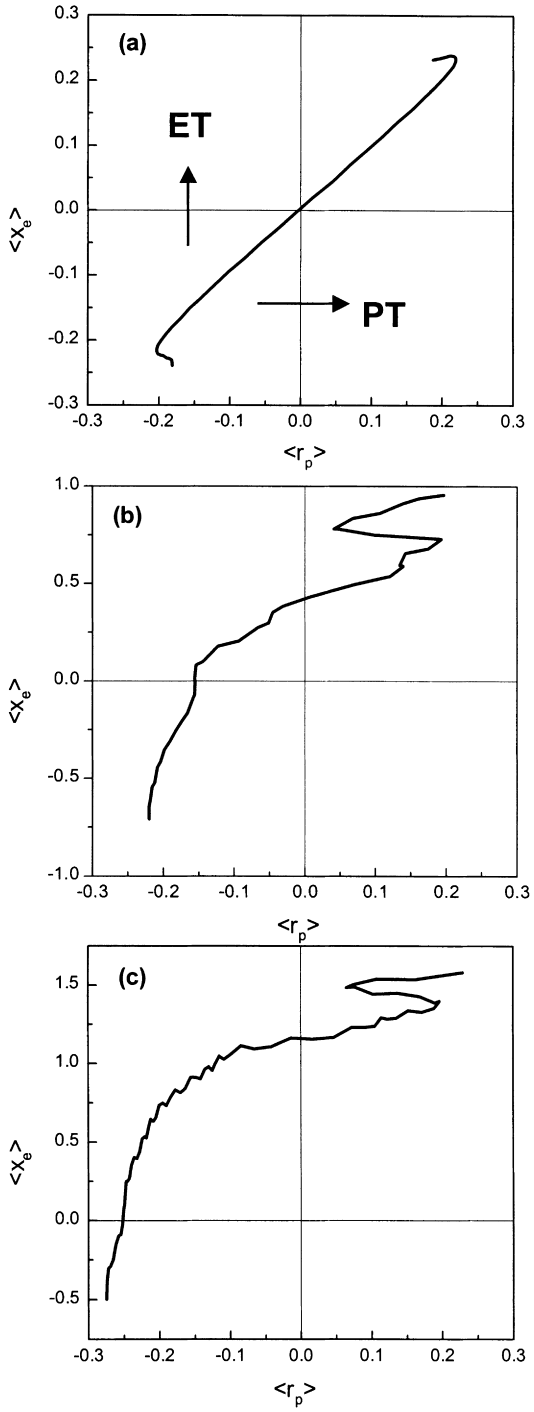

Fig. 9. Two-dimensional tunneling paths (as a function of the averaged positions of the proton ($\langle r_p \rangle$) and electron ($\langle x_e \rangle$), for (a) ET–PT, (b) PT → ET, and (c) ET → PT mechanisms. In (a) two different directions are denoted for PT and ET, respectively.

the results of calculations describing the dynamics of the proposed PT → ET mechanism.

Our results certainly do not completely rule out the possibility of a sequential PT → ET process. In order for PT to occur first, the proton needs sufficient time to search for an appropriate configuration before ET is induced. Such a mechanism requires a suppression of ET, which can be accomplished by using a smaller initial momentum for the solvent coordinate. In the present model, the sequential PT → ET process is possible on the ground state adiabatic surface (see Ref. [16], Fig. 8). Starting from the initial configuration, the system switches to the first excited state around $R_s = -0.45$. If the PCET reaction proceeds in the excited states, the actual mechanism will be of type ET → PT, as found in the present calculations. If most of the system is unable to pass the second barrier ($R_s \sim 0.25$) in the excited state and come back down to the first nonadiabatic transition region, it switches to the ground state, either going back to the reactant or resulting in the PCET reaction. The PCET reaction proceeding this way can have the suggested PT → ET mechanism. Since correct treatment of the bifurcation and coupling between adiabatic states is important, the present quantum/classical method may not be appropriate in such cases. It may be possible to obtain information on such a mechanism by examining the trajectories resulting from surface-hopping studies such as those using MDQT method. In any case, our results suggest that, for the sequential mechanism of coupled transfer, it is more probable for the electron to transfer first, thus providing a potential for the subsequent transfer of the proton.

As pointed out before, the validity of using the quantum/classical or Ehrenfest method for the specific problem studied in this paper needs to be evaluated. Studies of the limitations or range of applicability of the mixed quantum/classical method in a model system involving charge transfer such as PT or ET will be reported elsewhere. The present model system can also be used to test theoretical approaches for evaluating the rate constants of PCET reactions [13,14,19]. Such studies will help to elucidate the salient features of PCET reactions occurring in real systems.

Acknowledgements

This work was supported by the Basic Science Research Program (BSRI-97-3414) of the Ministry of Education, and by the S.N.U. Korea Electric Power Corp. Research Fund (96-15-1132).

References

[1] M.Y. Okamura, G. Feher, Ann. Rev. Biochem. 61 (1992) 861.
[2] G.T. Babcock, B.A. Barry, R.J. Debus, C.W. Hoganson, M. Atamian, L. McIntosh, I. Sithole, C.F. Yocum, Biochemistry 28 (1989) 9557.
[3] G.T. Babcock, M. Wikstrom, Nature 356 (1992) 301.
[4] B.G. Malmstrom, Acc. Chem. Res. 26 (1993) 332.
[5] E. Takahashi, P. Maroti, C. Wraight, in: A. Muller, H. Ratajczaks, W. Junge, E. Diemann (Eds.), Electron and Proton Transfer in Chemistry and Biology, Elsevier, Amsterdam, 1992, p. 219.
[6] T.A. Link, in: A. Muller, H. Ratajczaks, W. Junge, E. Diemann (Eds.), Electron and Proton Transfer in Chemistry and Biology, Elsevier, Amsterdam, 1992, p. 197.
[7] J.N. Onuchic, D.N. Beratan, J. Chem. Phys. 92 (1990) 722.
[8] M.J. Therien, M. Selman, H.B. Gray, I.-J. Chang, J.R. Winkler, J. Am. Chem. Soc. 112 (1990) 2420.
[9] C. Turro, C.K. Chang, G.E. Leroi, R.I. Cukier, D.G. Nocera, J. Am. Chem. Soc. 114 (1992) 4013.
[10] J.A. Roberts, J.P. Kirby, D.G. Nocera, J. Am. Chem. Soc. 117 (1995) 8051.
[11] R.I. Cukier, J. Phys. Chem. 98 (1994) 2377.
[12] R.I. Cukier, J. Phys. Chem. 99 (1995) 945.
[13] R.I. Cukier, J. Phys. Chem. 99 (1995) 16 101.
[14] R.I. Cukier, J. Phys. Chem. 100 (1996) 15 428.
[15] R.I. Cukier, J. Zhu, J. Phys. Chem. 101 (1997) 7180.
[16] J.Y. Fang, S. Hammes-Schiffer, J. Chem. Phys. 106 (1997) 8442.
[17] J.Y. Fang, S. Hammes-Schiffer, J. Chem. Phys. 107 (1997) 5727.
[18] J.Y. Fang, S. Hammes-Schiffer, J. Chem. Phys. 107 (1997) 8933.
[19] S. Shin, H. Metiu, J. Chem. Phys. 102 (1995) 9285.
[20] J.C. Tully, J. Chem. Phys. 93 (1990) 1061.
[21] S. Hammes-Schiffer, J.C. Tully, J. Chem. Phys. 101 (1994) 4657.
[22] N.P. Blake, V. Srdanov, G.D. Stucky, H. Metiu, J. Phys. Chem. 99 (1995) 2127.
[23] J. Ka, S. Shin, Chem. Phys. Lett. 269 (1997) 227.
[24] S. Shin, H. Metiu, J. Phys. Chem. 100 (1996) 7867.
[25] R.J. Kuntz, J. Chem. Phys. 95 (1991) 141.
[26] D. Kohen, F.H. Stillinger, J.C. Tully, J. Chem. Phys. 109 (1998) 4713.